with theory, but at lower temperatures the theoretical behavior of $\kappa_2(t)$ has not yet been worked out. Experimentally, $\kappa_2(t)/\kappa$ for this sample of vanadium is considerably higher than for the case of alloy superconductors,[7,48] which is in qualitative agreement with theory and with results of niobium.[7] This work has also shown that calorimetric measurements can be used to give a reliable estimate of the Fermi surface area by using Eq. (26), which in turn allows accurate calculations to be made for several other electronic parameters.

## ACKNOWLEDGMENT

We are grateful to Dr. G. A. Alers of the Ford Scientific Laboratory for loaning us the vanadium sample and for bringing this problem to our attention.

PHYSICAL REVIEW VOLUME 149, NUMBER 1 9 SEPTEMBER 1966

# Superconducting Properties of High-Purity Niobium*

D. K. FINNEMORE, T. F. STROMBERG,† AND C. A. SWENSON
*Institute for Atomic Research and Department of Physics, Iowa State University, Ames, Iowa*
(Received 7 March 1966)

Precision magnetization data are given for high-purity niobium metal samples (resistance ratio $R_{300}/R_{4.2}{}^N = 1600 \pm 400$) over the range from 1.1°K to $T_c = 9.25(\pm.01)$°K. The thermodynamic critical-field curve, which is parabolic to 1%, is that to be expected for an intermediate-coupling superconductor. The magnetization curves are qualitatively like those associated with a type-II superconductor with $\kappa \sim 1$, but the detailed shape does not follow any theory. In particular, the magnetization increases linearly with a slope of 23 G/Oe from 1.005 $H_{c1}$ to 1.025 $H_{c1}$, where a sharp break occurs to a smaller slope. The magnetization data at $H_{c1}$ and in the region of $H_{c2}$ are consistent with published specific-heat data. The magnitudes of $H_{c2}$ and $H_c$ are consistent with measured values of the penetration depth $\lambda$. Preliminary data are reported for $H_{c3}$ as obtained from both resistive and ac susceptibility measurements.

## I. INTRODUCTION

THE superconducting properties of transition metals such as niobium, tantalum and vanadium generally have been defined quite poorly when compared with nontransition metals like tin, indium, and mercury.[1] The transition metals were believed to belong to a class of materials (which includes most alloys) which show nonideal irreversible superconducting transitions and considerable irreproducibility from sample to sample.[2] In contrast, the nontransition metals can be prepared so as to give well-defined and reproducible superconducting transitions. The arbitrariness of this distinction was emphasized when investigations of the superconducting properties of extremely high-purity tantalum[3,4] metal showed the ideal superconducting behavior which formerly was associated with the softer materials.

Our initial objective was to establish that the superconducting behavior of high-purity niobium metal was similar to that of high-purity tantalum. Our preliminary results, however, showed quite different types of magnetization curves for equivalent samples (that is, the same resistance ratio and long, thin shape) of the two metals.[5] For tantalum, complete flux penetration took place over a very narrow region of applied magnetic field, while for niobium the flux penetration was spread over a much wider range of magnetic fields. The magnetization behavior was reversible in both cases, with no locked-in flux. Resistive transition data also suggested a fundamental difference for niobium.[6] Similar effects have been observed in alloys, and these can be understood in terms of arguments advanced by Pippard[7] and a theory due to Ginzburg and Landau,[8] Abrikosov[9] and Gor'kov[10] (GLAG). These ideas can be discussed in terms of the magnetic field penetration depth $\lambda$ which is a measure of the depth of penetration of surface currents on a superconducting sample, and the coherence length $\xi$ which is characteristic of the range of order in the superconducing state. As Pippard[7] has pointed out, the excess surface free energy between

* Work was performed at the Ames Laboratory of the U. S. Atomic Energy Commission. Contribution No. 1753.
† Present address: Los Alamos Scientific Laboratory, Los Alamos, New Mexico.
[1] D. Shoenberg, *Superconductivity* (Cambridge University Press, New York, 1952), 2nd ed.
[2] A. Calverley, K. Mendelssohn, and P. M. Rowell, Cryogenics **2**, 26 (1961).
[3] D. P. Seraphim, D. T. Novak, and J. I. Budnick, Acta Met. **9**, 446 (1961).
[4] C. H. Hinrichs and C. A. Swenson, Phys. Rev. **123**, 1106 (1961).
[5] T. F. Stromberg and C. A. Swenson, Phys. Rev. Letters **9**, 370 (1962).
[6] S. H. Autler and E. S. Rosenblum, Phys. Rev. Letters **9**, 489 (1962).
[7] A. B. Pippard, Proc. Cambridge Phil. Soc. **47**, 617 (1951); Proc. Roy. Soc. (London) **A216**, 547 (1953).
[8] V. L. Ginzburg and L. D. Landau, Zh. Eksperim. i Teor. Fiz. **20**, 1064 (1950).
[9] A. A. Abrikosov, Zh. Eksperim. i Teor. Fiz. **32**, 1442 (1957) [English transl.: Soviet Phys.—JETP **5**, 1174 (1957)].
[10] L. P. Gor'kov, Zh. Eksperim. i Teor. Fiz. **37**, 1407 (1959) [English transl.: Soviet Phys.—JETP **10**, 998 (1960)].

superconducting and normal regions in a sample depends directly on the relative magnitudes of these two quantities. If $\xi \gg \lambda$, this free-energy contribution is positive and a configuration of normal and superconducting regions cannot be stable except near the critical field in the intermediate state. This class of superconductors (which includes the high-purity nontransition metals) shows sharp transitions at a magnetic field, $H_c$, and has been designated as type I. If $\xi \ll \lambda$, however, the surface free-energy contribution is negative and for a given value of the applied magnetic field the free energy may be reduced by allowing flux penetration and the formation of normal superconducting boundaries. These negative surface free-energy or type-II superconductors[11] generally are found in alloy systems where electron scattering results in a reduction in the coherence length $\xi$.[12]

There are at least three distinct critical fields associated with type-II superconductors. The thermodynamic critical field $H_c$ is defined for both type-I and type-II superconductors in terms of the zero-magnetic-field free-energy difference between the normal and superconducting states and can be obtained either from specific-heat or from reversible magnetization-curve measurements.[1] At low magnetic fields, both type-II and type-I superconductors exhibit a perfect Meissner effect; that is, the magnetic flux is completely excluded from the sample. As the magnetic field is increased, surface free-energy effects become important for type-II superconductors and partial flux penetration occurs abruptly at a value of the applied magnetic field $H_{c1}$ which is less than $H_c$. In this case, the superconducting state persists in magnetic fields greater than $H_c$, and flux penetrates the sample completely at a third critical field $H_{c2}$.

The original theory (GLAG)[8–10] which is applicable only near the critical temperature $T_c$ has been extended to all temperatures for the short-mean-free-path case by Maki.[13] The long-mean-free-path limit which applies to niobium has been studied, also with results which apply only near $H_{c2}$.[14] No theory exists, however, for the long-mean-free-path limit over the entire range of temperature and magnetic field. It is customary in work of this type to introduce the Ginzburg-Landau parameter $\kappa = H_{c2}/\sqrt{2}H_c$ (see Refs. 9, 10) or the Maki parameters $\kappa_1$ and $\kappa_2$ (Ref. 13) in a description of the data. In situations where the theories apply, these parameters can be related directly to the experimentally measured variables and are very useful. For niobium, however, the theories do not apply very well and most of our discussion will be presented directly in terms of the measured quantities.

The present work confirms and extends our original observation that very pure niobium is a type-II superconductor for which $\lambda \sim \xi$.[5] In particular, an effort has been made to provide reliable determinations of the variation in the shape of the magnetization curve with temperature and the temperature dependences of the various critical fields. The high zero-field transition temperature $T_c = 9.25$°K of niobium makes it possible to work conveniently over a wide range of reduced temperatures; 1.1 to 9.25°K corresponds to reduced temperatures $t = T/T_c$ of 0.12 to 1.0. The experimental situation for niobium is complicated by the sensitivity of the superconducting properties to small amounts of dissolved gases.[3,15] Despite this sensitivity the specific-heat,[16–18] the electron-tunneling energy-gap,[19,20] the ultrasonic-attenuation,[21] and the critical-current[6] measurements give a reasonably consistent picture when variations in sample purity are considered. Quantitative studies by DeSorbo[15] have shown that $T_c$ can be decreased by as much as 0.5°K by dissolved oxygen or increased by a similar amount by strain. The wide variations in both transition temperature and critical field reported in the literature probably are due to effects such as these. Hence, we have taken great care to remove dissolved gases and strains from initially high-purity niobium, and have produced samples of small diameter with residual resistivity ratios $[\Gamma = R_{300}/R_{4.2}{}^N]$ ranging from 1200 to 2000. These samples show less than 1% variation in critical fields from sample to sample, and almost complete reversibility in the magnetization curves. The data which we present below furnish a rigorous test of theories which should be applicable to high-purity (long-mean-free-path) type-II superconductors over a wide range of temperatures.

## II. EXPERIMENTAL

### Sample Preparation

The initial niobium metal was obtained from the DuPont Corporation in the form of granules of about $\frac{1}{32}$ in. diam. Typical chemical analyses of the original material (which show the very low metallic-impurity content) and the final material used in these measurements are shown in Table I, where it can be seen that the major metallic impurity is roughly 175 parts per

[11] B. B. Goodman, Phys. Rev. Letters **6**, 597 (1961); IBM J. Res. Develop. **6**, 63 (1962).

[12] These ideas are discussed at some length by various authors in the Proceedings of the International Conference on the Science of Superconductivity, 1963, which appeared in Rev. Mod. Phys. **36**, No. 1 (1964).

[13] K. Maki, Physics **1**, 21 (1964); **1**, 127 (1964).

[14] E. Helfand and N. R. Werthamer, Phys. Rev. Letters **13**, 686 (1964); K. Maki and T. Tsuzuki, Phys. Rev. **139**, A868 (1965); L. Neumann and L. Tewordt, Z. Physik **191**, 73 (1966).

[15] W. DeSorbo, Phys. Rev. **130**, 2177 (1963); **132**, 107 (1963); **134**, A1119 (1964); **135**, A1190 (1964).

[16] B. J. C. van der Hoeven and P. H. Keesom, Phys. Rev. **134**, A1320 (1964).

[17] H. A. Leupold and H. A. Boorse, Phys. Rev. **134**, A1322 (1964).

[18] L. Shen, N. M. Senozan, and N. E. Phillips, Phys. Rev. Letters **14**, 1025 (1965).

[19] M. D. Sherrill and H. H. Edwards, Phys. Rev. Letters **6**, 460 (1961).

[20] P. Townsend and J. Sutton, Phys. Rev. **128**, 591 (1962).

[21] E. R. Dobbs and J. M. Perz, Rev. Mod. Phys. **36**, 257 (1964); R. Weber, Phys. Rev. **133**, A1487 (1964).

TABLE I. Typical chemical analysis for several niobium samples.

| Sample | O | N | H | C | Ta | Fe | Ce | Ni | W |
|---|---|---|---|---|---|---|---|---|---|
| As received | 64 | 1 | 80 | 13 | 175 | <50 | <30 | <30 | <50 |
| Outgassed | 6–16 | 8 | 1 | 40 | 175 | <50 | <30 | <30 | <50 |

million (ppm) tantalum. The variations in carbon content are believed to be within the limits of the error of the analytical methods used. Cylindrical wire specimens were formed by arc melting the granules in an argon atmosphere, electron-beam melting the resulting button in a vacuum of $10^{-6}$ Torr, arc melting again in an argon atmosphere into a cylindrical shape, and then swaging this cylinder into a wire before it was drawn into the final diameter. Contamination with carbon from the pump oil and the swaging lubricant appeared to be less than 40 ppm at this stage, and before further processing the surface of the wire was cleaned with boiling sulfuric acid. As was done for tantalum, dissolved gases such as nitrogen, oxygen, and hydrogen were removed by outgassing wires which are approximately 4 in. long and 0.020 in. in diam. in a vacuum of $10^{-9}$ Torr at a temperature approximately 50°C below the melting point for periods of 8 to 12 h.[3,4] We find that electron-beam heating gives the most uniform temperature along the wire and have applied this method to all of the samples used in this research. The analysis for an "outgassed" sample in Table I shows the reduction in gaseous content. An attempt was made to reduce the carbon content of some of the samples by "soaking" them in an oxygen atmosphere of $10^{-5}$ Torr for 10 min near the melting point.[3,4] There is no obvious improvement in the properties of the samples. After the samples were outgassed, they were removed from the furnace, glued to a brass block with Duco cement and cut into sections approximately 0.5 in. long for magnetization measurements. Acetone was used to remove the Duco cement. After the magnetization data were taken, the normal-state electrical resistivity at 4.2°K was determined in a field of 6000 Oe by measuring the voltage drop across the sample due to currents of 0.1 to 1.0 A. Razor blade potential probes were used. Resistivity ratios for the samples used in experiments reported here are shown in Table II. Approximately one-half of the samples

TABLE II. Resistivity ratios for several niobium samples.

| Sample | Treatment | Γ | Diameter (in.) |
|---|---|---|---|
| Nb-33-1 | Heated without $O_2$ | 2080 | 0.025 |
| Nb-33-2 | Heated without $O_2$ | 2050 | 0.025 |
| Nb-32-3 | Heated with $O_2$ | 1670 | 0.025 |
| Nb-35-3 | Heated with $O_2$ | 1830 | 0.025 |
| Nb-49 | Heated without $O_2$ | 1360 | 0.015 |
| Nb-44-3 | Heated without $O_2$ | 1480 | 0.020 |
| Nb-53-2 | Heated without $O_2$ | 1490 | 0.025 |
| Nb-53-3 | Heated without $O_2$ | 1670 | 0.025 |
| Nb-48-1 | Heated without $O_2$ | 1360 | 0.020 |

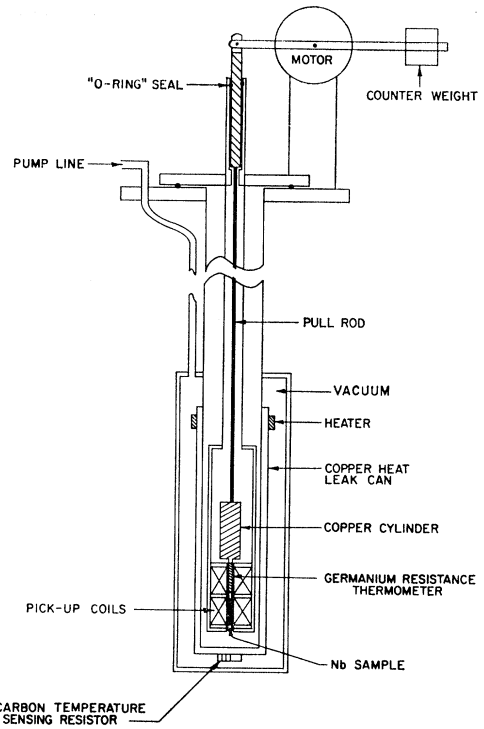


FIG. 1. Sample-motion magnetometer for temperatures above 4.2°K. The surrounding liquid-helium and liquid-nitrogen baths are not shown.

prepared and treated in this fashion have Γ's greater than $10^3$, and the highest Γ which we have observed is 2200. The differences between various samples are not understood, although there is some indication that the smaller diameter wires are more easily deformed in the resistivity ratio measurement and, hence, show too low a value. It must be emphasized that the resistivity ratios were determined after the magnetization data were taken, and that the samples on which data were taken were at least this good.

### Cryostat

All of the magnetization measurements presented here were made by moving the sample by 2 cm in a uniform magnetic field between two counter-wound 26 000-turn pick-up coils, and noting the resulting deflection of a ballistic galvanometer (Leeds and Northrup, Model 2285-X, CDRX 960 Ω). The magnetic field was provided by a liquid-nitrogen-cooled copper solenoid which is homogeneous to 0.01% over a distance of 4 cm along the axis. The maximum fields available were roughly 4000 Oe and were limited by the current-regulated power supply which was available. The solenoid calibration is based on the proton resonance in glycerine, while its homogeneity is that determined using a mutual-inductance technique. The earth's field was compensated to approximately 0.01 Oe by a Helmholtz coil arrangement.

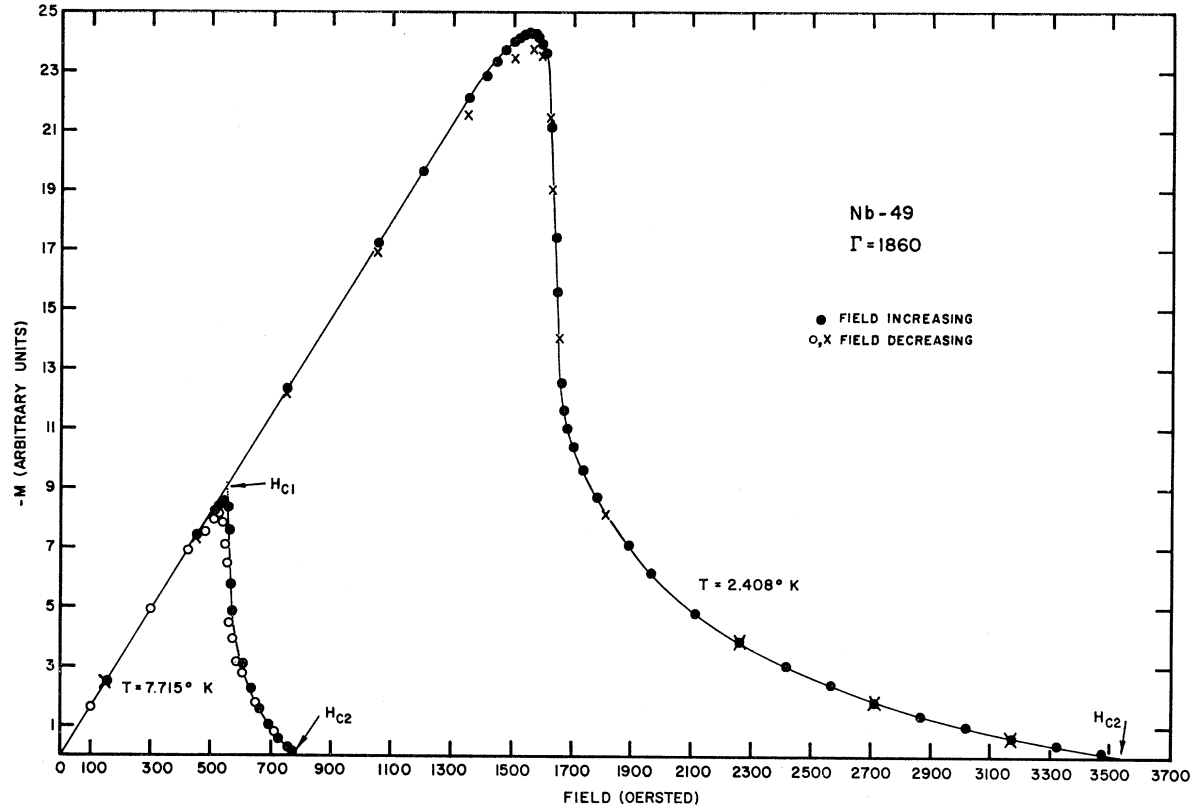


FIG. 2. Reversible magnetization curves at two different temperatures for Nb 49. $\Gamma = 1360$.

Two separate cryostats were used for the magnetization measurements, one for temperatures from the normal boiling point of helium down to 1.1°K, and one for higher temperatures. The sample was immersed in the liquid helium in the first apparatus, and was assumed to be at the temperature of the surrounding liquid. The vapor pressure was used together with the *T*-58 helium vapor pressure scale[22] to determine the temperature of the liquid; above 2.2°K, the vapor pressure was that measured in a vapor pressure bulb located close to the sample (to minimize hydrostatic head effects), while below 2.2°K the vapor pressure was measured directly over the liquid surface. In this apparatus the sample was connected by means of a copper wire and a stainless-steel capillary to the iron core of a solenoid at room temperature. The sample was moved between the coils as the solenoid was energized. The sample motion was quite violent, but the magnetization data indicate no motion-induced sample heating.

The apparatus designed for work above 4.2°K (Fig. 1) differs from the one just described in several respects, since a heat-leak chamber must be used, and heating effects due to rapid sample motion were found to be large. The sample and a germanium resistor were encased in a 2 in. long, $\frac{3}{16}$ in. diam. high-purity copper sleeve which was attached to a "massive" copper cylinder (Fig. 1). This whole assembly was driven smoothly between the two coils by means of a reversing motor located on top of the cryostat at room temperature. The time of the motion (roughly $\frac{1}{4}$ sec) was small compared with the period of the ballistic galvanometer (11.2 sec). Unless great care is taken to provide smooth motion, vibration can cause uncertainties in the sample temperature as great as 0.05°K. This effect is a maximum at low temperatures where the heat capacity of the copper sleeve is small and is negligible near 9°K. The heat-leak chamber which surrounds the sample-holder–thermometer combination consisted of a large copper shield which was isolated from the helium bath by type 321 stainless-steel tubing. A carbon-resistor sensing thermometer and a noninductive manganin heater were mounted on the copper shield to provide a constant-temperature region around the entire assembly. Data taken with this cryostat join smoothly and overlap the data taken with the other cryostat.

The secondary thermometer used above 4.2°K is a series II Honeywell germanium resistor which has been calibrated with a constant-volume gas thermometer. Details of the calibration have been reported else-

[22] H. van Dijk, M. Durieux, J. R. Clement, and J. K. Logan, J. Res. Natl. Bur. Std. 64A, 4 (1960).

where.[23,24] As a check on our thermometry, we find the zero-field superconducting transition temperature of a high-purity lead sample to be 7.195°K, in good agreement with the value reported by Franck and Martin,[25] 7.193°K.

## III. RESULTS AND DISCUSSION

Magnetization data were taken for both increasing and decreasing magnetic fields at various temperatures between 1.1 and 9°K. Typical magnetization data are shown in Fig. 2 for one sample (Nb 49) at two different temperatures.[26] The solid dots indicate the virgin magnetization curve (that is, the sample was warmed to a temperature considerably above 9°K and then cooled in zero magnetic field before these data were taken), while the other symbols refer to a decrease in the magnetic field. The definitions which we use for both $H_{c1}$ and $H_{c2}$ are shown. As will be discussed below, the curvature near $H_{c1}$ does not appear to be an end effect. In general, the magnetization curves show hysteresis which varies in a nonsystematic manner from sample to sample and also from one temperature to another for a given sample which has been kept at a temperature below 20°K. These effects are present even when no locked-in flux (at zero magnetic field) is observed. This hysteresis is most marked in the $H_{c1}$ region where $H_{c1}$ as determined from the virgin magnetization curve and from the subsequent decrease in magnetic field might differ by anywhere from 1–5%. The value of $H_{c1}$ as determined by a subsequent increase of field can be less than the virgin value by as much as 1%. The consistent feature of data taken for many different samples with varying lengths, diameters, resistivity ratios, etc., appears to be the virgin magnetization curve. Hence, all of the magnetization data reported below were taken only after the sample was warmed above 9°K and cooled to the given temperature in zero magnetic field. Samples which showed detectable locked-in flux at 4.2°K (of the order of $\frac{1}{2}$% of the maximum magnetization) were rejected immediately.

Consistent values of the magnetization were obtained for fields just above $H_{c1}$ only after the sample had been moved between the coils a number of times. The change in the magnetization of a sample upon a slight increase (or decrease) of the field is very dependent on the fact that the sample has been jarred as it is pulled between the measuring coils, and a final, steady-state value of the magnetization is sometimes obtained only after 10 or 20 sample translations. It is as if vibration assists the flux movement into or out of the sample. Hence, all of the data reported below refer to the final steady state of the magnetization; that is, further sample motion would produce no further change.

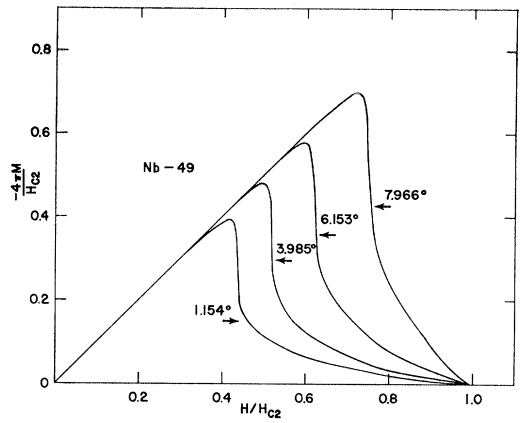


FIG. 3. A comparison of the shapes of the magnetization curves as a function of temperature. The ordinate and abscissa are scaled by $H_{c2}$.

The general shape of the magnetization curves for Nb (Figs. 3–5) is similar to the behavior described by Abrikosov[9] and Goodman,[11] but a detailed study shows that there are important distinctions. To facilitate discussion, we have followed Abrikosov in defining $H_{c1}$ as the field of initial flux penetration, $H_{c2}$ as the field at which the magnetization first reaches the normal state value,[9] and $H_c$ as the field related to the free energy for a long, thin sample by

$$G_n - G_s = \frac{VH_c^2}{8\pi} = -V\int_0^{H_{c2}} M\,dH, \qquad (1)$$

where $G_n$ and $G_s$ are the magnetic Gibbs free energy in the normal and superconducting states. At low fields the flux exclusion is complete and the magnetization has the form $M=-\frac{1}{4}\pi H$. At fields just above $H_{c1}$, the magnitude of $M$ decreases rapidly until it has dropped by a factor of 2, and in this region the curve is linear within the accuracy of our measurement. At higher fields, $|M|$ decreases gradually until it reaches the normal-state value at $H_{c2}$. The identification of $H_{c1}$ from these data requires some judgement because the break in the curve is not sharp. The data show, however, that an extrapolation of the two linear portions of the curve as shown in Fig. 2 gives $H_{c1}$ values which are independent of sample geometry and reproducible from sample to sample. On the basis of these facts, we identify the magnetic field of this intersection to be $H_{c1}$.

As the temperature is lowered below the critical temperature, the shape of the magnetization curves changes in a regular way. Figure 3 illustrates these variations on a reduced plot. The ordinate and abscissa have been scaled by $H_{c2}$ to emphasize deviations from similarity. Both the $H_{c1}/H_{c2}$ ratio and the slope at

[23] D. K. Finnemore, J. E. Ostenson, and T. F. Stromberg, U. S. Atomic Energy Commission Report IS-1046 (unpublished).

[24] D. K. Finnemore, D. L. Johnson, J. E. Ostenson, F. H. Spedding, and B. J. Beaudry, Phys. Rev. **137**, A550 (1965).

[25] J. P. Franck and D. L. Martin, Can. J. Phys. **39**, 1320 (1961).

[26] The actual experimental data which were obtained for the magnetization curves are given by T. F. Stromberg, Ph.D. thesis, Iowa State University, 1965 (unpublished). These data are available upon request to either D. K. Finnemore or C. A. Swenson, Physics Division, Ames Laboratory USAEC, Ames, Iowa 50010.

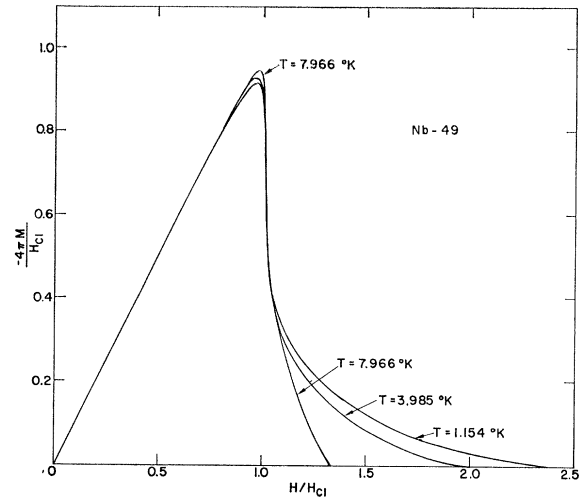


FIG. 4. A comparison of the shapes of the magnetization curves as a function of temperature. The ordinate and abscissa are scaled by $H_{c1}$ to show the similarity in the region of $H_{c1}$.

$H_{c2}$ decrease with decreasing temperature, but the slope at fields just above $H_{c1}$ is surprisingly constant. An alternate presentation which emphasizes the similarity of the curves is shown in Fig. 4 where the ordinate and abscissa are normalized by $H_{c1}$. In the region just above $H_{c1}$ the negative reduced magnetization $(-4\pi M/H_{c1})$ drops abruptly with a slope which is independent of temperature for all temperatures less than 8°K. At higher temperatures this slope decreases by approximately 20%. Another feature is illustrated in Fig. 4 as the systematic change in the rounding of the curves just below $H_{c1}$. As the temperature increases the rounding decreases and the intial penetration of flux into the sample becomes substantially more abrupt. Each of these features has implications for our understanding of the type-II behavior of niobium and will be discussed in more detail.

### Thermodynamical Critical Field $H_c$

The temperature dependence of the thermodynamic critical-field curve [Eq. (1)] is close to that found for type-I superconductors despite the fact that the magnetization curves are broad. Figure 5 shows that the data for three different samples closely follow a parabolic critical-field curve of the form $H_c=H_0(1-t^2)$, where $t=(T/T_c)$. The scatter of the data for a given sample and the scatter from sample to sample are approximately 1%, although one would expect better precision than this from the data for a given magnetization. Smoothed values of $H_c$ are given as a function of $t^2$ (with $T_c=9.25$°K) in Table III.

The value of $H_0$ may be obtained most reliably by making use of the form of the critical field curve which must apply at low temperatures where the superconducting entropy is much smaller than the normal

TABLE III. A smoothed summary of various niobium magnetization data. $t=T/T_c$, with $T_c=9.25$°K. $\kappa_1$ and $\kappa_2$ are defined in the text.

| $t^2$ | $H_c$ Oe | $H_{c1}/H_c$ | $\kappa_1$ | $\kappa_2$ | $-4\pi\frac{dM}{dH}\Big\vert_{H_{c2}}$ G/Oe |
|---|---|---|---|---|---|
| 0 | (1993) | (0.871) | (1.43) | (2.98) | (0.05) |
| 0.1 | 1796 | 0.883 | 1.32 | 2.24 | 0.10 |
| 0.2 | 1598 | 0.892 | 1.22 | 1.90 | 0.14 |
| 0.3 | 1401 | 0.899 | 1.14 | 1.67 | 0.19 |
| 0.4 | 1196 | 0.904 | 1.08 | 1.49 | 0.25 |
| 0.5 | 997 | 0.909 | 1.02 | 1.34 | 0.33 |
| 0.6 | 793 | 0.913 | 0.97 | 1.21 | 0.44 |
| 0.7 | 592 | 0.917 | 0.92 | 1.10 | 0.59 |
| 0.8 | 395 | 0.921 | 0.87 | 0.99 | 0.86 |
| 0.9 | 197 | 0.923 | 0.82 | 0.88 | 1.51 |
| 1.0 | 0 | (0.925) | (0.78) | (0.78) | (4.06) |

entropy[27]

$$H_c^2=H_0^2-(4\pi\gamma/V)T^2, \tag{2}$$

where $\gamma$ is the normal-state electronic specific-heat coefficient, and $V$ is the molar volume. An analysis such as this for our data gives $H_0=1993\pm10$ Oe and $\gamma=7.9^5(\pm0.2)$ mJ/mole °K using $V=10.8$ cm$^3$/mole.[17] The actual data can best be represented in a deviation of the data from parabolic behavior by means of the function

$$D(t)=(H_c/H_0)-(1-t^2), \tag{3}$$

and this deviation plot is given in Fig. 6. The parabolic nature of the data is clearly shown, and it is possible to use the assumption of a parabolic critical-field curve to obtain directly a value of $\gamma=8.0(\pm0.2)$ mJ/mole °K using the above values of $H_0$, $T_c$, and $V$. Both of these results are in agreement with the recent calorimetric work of Leupold and Boorse ($\gamma=7.80$ mJ/mole °K),[17]

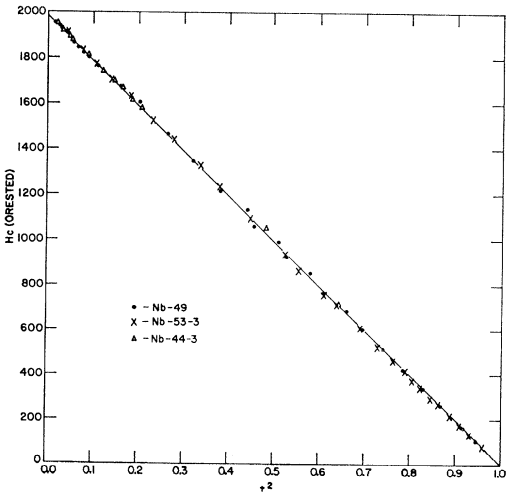


FIG. 5. Thermodynamic critical-field $[H_c(T)]$ data for niobium.

[27] J. E. Schirber and C. A. Swenson, Phys. Rev. **123**, 1115 (1961).

van der Hoeven and Keesom ($\gamma=7.79$ mJ/mole °K),[16] and Shen, Senozan, and Phillips ($\gamma=7.85$ mJ/mole °K).[18]

Several methods have been used to determine $T_c$ for these samples. The extrapolation to zero of the critical fields $H_c$, $H_{c1}$, or $H_{c2}$ as well as a direct zero-field determination by a 33-cps ac susceptibility technique all give $T_c=9.25\pm0.01$°K. This value agrees well with the value of 9.25°K given by Phillips[18] but is somewhat higher than the value of 9.19°K given by Leupold and Boorse.[17] This discrepancy may be due to gaseous contamination in the samples used in the specific-heat work.

We also can relate the slope of the critical-field curve at $T_c$ to the jump in specific heat by the relationship[1]

$$\Delta C=C_n-C_s=\frac{VT_c}{4\pi}\left(\frac{dH_c}{dT}\right)^2_{T=T_c}. \quad (4)$$

The magnetization data give $\Delta C=147$ mJ/mole °K, which is to be compared with the calorimetric values of 134 mJ/mole °K[17] and 130 mJ/mole °K.[16] It is not clear why this discrepancy is larger than the corresponding differences in $H_0$ and $T_0$, although some rounding could appear in the direct determinations.

For the case of type-I superconductors, such as Sn or Hg, the measured quantities $H_0$, $T_c$, and $\gamma$ can be related to one another and to the superconducting energy gap by the theory of Bardeen, Cooper, and Schrieffer (BCS).[28,29] It is of interest to use these parameters for a type-II superconductor to test the generality of the BCS relations. The energy gap as calculated from[28]

$$\Delta=H_0\left(\frac{\pi k^2V}{6\gamma}\right)^{1/2} \quad (5)$$

is $3.66kT_c$ compared with the BCS value of $3.52kT_c$. This also compares favorably with the electron tunneling values of $3.59\ kT_c$[19] and $3.84\ kT_c$[20] or the ultrasonic values of 3.6 to 3.7 $kT_c$.[21] To display a comparison with the theory over the entire range, it is convenient to compare the deviation of the data and the theory from a parabolic critical-field curve using Eq. (3). This comparison (Fig. 6) shows that the data for niobium lie between the curves for tin and mercury,[30] with $D(t)$ being almost zero. Among type-I superconductors there is a strong correlation between the ratios $(T_c/\Theta_D)$ and $(2\Delta/kT_c)$ (shown in Table IV) and the shape of the deviation function. Low values of $(T_c/\Theta_D)$ give a negative $D(t)$ (see tin in Fig. 6), while larger values of this quantity are associated with a positive $D(t)$ (as for mercury).[30] Within the theory, these effects are related to the coupling between electrons through the phonons.[31] Niobium fits this general trend and might be described as an intermediate-coupling superconductor which has a bulk free energy reasonably close to the predictions of BCS.

TABLE IV. Correlations between the → energy gap parameter and the coupling parameter for various superconductors.[a]

| Metal | $T_c/\Theta_D$ | $2\Delta/kT_c$ |
|---|---|---|
| Al | 0.003 | 3.2 |
| BCS | 0 | 3.52 |
| Sn | 0.019 | 3.60 |
| In | 0.031 | 3.64 |
| Nb | 0.037 | 3.66 |
| Hg | 0.052 | 3.96 |
| Pb | 0.076 | 3.95 |

[a] See Ref. 30.

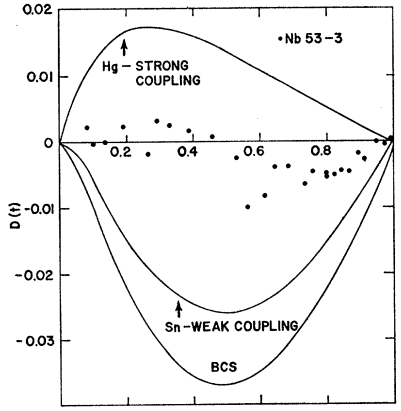


FIG. 6. A deviation function plot for niobium, tin, mercury, and BCS. $D(t)=(H_c/H_0)-(1-t^2)$.

### The Lower Critical Field $H_{c1}$

The type-II character of niobium requires an extension or modification of BCS. At present there is no adequate theory for a very pure type-II superconductor over the entire temperature range, but the Abrikosov model provides a good starting point for such an extension. The discussion here will be cast in terms of this model in an attempt to establish more clearly its range of validity. Our data for the temperature dependence of $H_{c1}$ are shown in Fig. 7, and smoothed values of $H_{c1}/H_c$ are given in Table III. A purely empirical relationship which represents the data to an accuracy of 1%

$$H_{c1}=1735(1-t^{2.13})\ \text{Oe}$$

is shown by the solid line on the Fig. 7. Other criteria than those shown in Fig. 2 can be used to determine $H_{c1}$ from the magnetization curves, but these would not substantially alter the temperature dependence.

[28] J. Bardeen, L. N. Cooper, and J. R. Schrieffer, Phys. Rev. **108**, 1175 (1957).

[29] J. Bardeen and J. R. Schrieffer, in *Progress in Low Temperature Physics* (North-Holland Publishing Company, Amsterdam, 1961), Vol. III.

[30] D. K. Finnemore and D. E. Mapother, Phys. Rev. **140**, A507 (1965).

[31] J. C. Swihart, D. J. Scalapino, and Y. Wada, Phys. Rev. Letters **14**, 106 (1965).

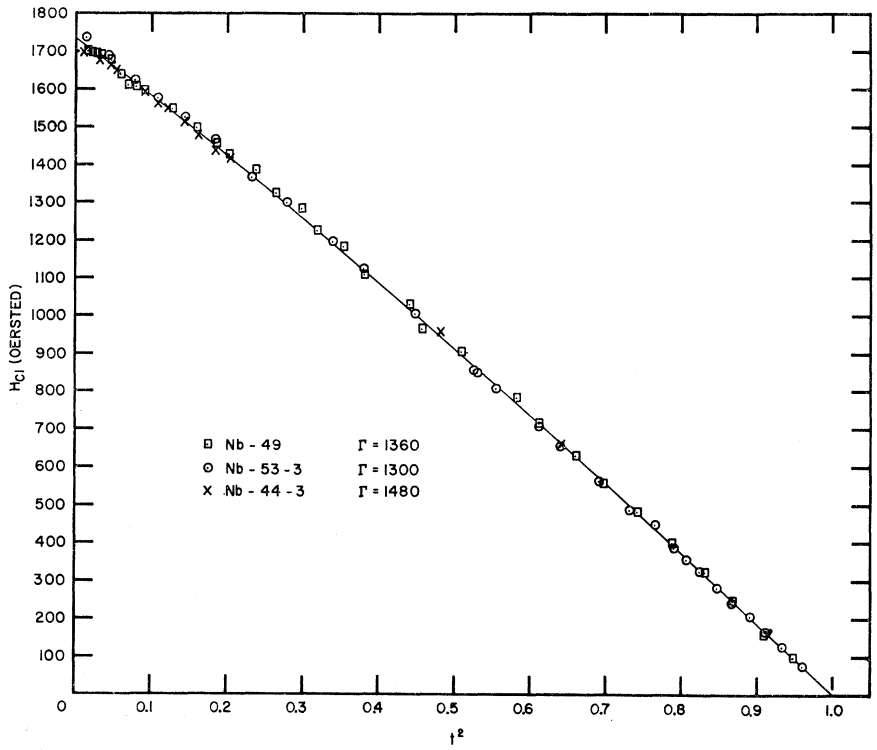


FIG. 7. Lower critical-field ($H_{c1}$) data for niobium. The data deviate above a parabolic temperature dependence by approximately 5%.

The detailed nature of the phase transition at $H_{c1}$ has been the subject of considerable discussion. Within the framework of the Abrikosov model,[9] a first-order transition is expected when, like in niobium, $H_{c2}$ is comparable with $H_{c1}$. More recent theoretical work by Matricon[32] and Goodman[33] based on a vortex model suggests a λ-type anomaly in the specific heat and for fields slightly greater than $H_{c1}$ a $B$-versus-$H$ relationship of the form

$$[(H-H_{c1})/H_{c1}]=a\exp[c(H_{c1}/B)^{0.5}], \qquad (6)$$

where $a$ and $c$ are constants and $B$ is the magnetic induction. While the nature of such a transition can be discussed easily from a theoretical standpoint, it often is difficult to establish this shape experimentally.

McConville and Serin[34] have presented both specific-heat and magnetization data for niobium which suggest a λ transition at $H_{c1}$. Such interpretations are somewhat ambiguous, however, since the finite dimensions of the sample always must give a finite width to magnetic transition due to demagnetizing fields, and any deviation of the sample geometry from elliptical shape will produce magnetic field inhomogeneities which in turn will broaden the transition even further. Hence, one must make an interpretation of the data at fields which are not too close (1 or 2% for the case of Serin's data) to $H_{c1}$ and then extrapolate back to $H_{c1}$. The added difficulty exists for niobium that it is difficult to produce samples of sufficient chemical and mechanical perfection to guarantee homogeneous behavior. Each of these criticisms will be investigated with respect to the results presented here.

We have taken data on a large number of samples over a wide range of temperatures, and all of the results indicate a linear relationship between $M$ and $H$ for fields slightly greater than $H_{c1}$. The magnitude of the slope (23 G/Oe) is nearly independent of the temperature (±15%), although it appears to drop to approximately 16 G/Oe at temperatures above 8.5°K. These slopes are at least ten times smaller than those to be expected from the demagnetization factors if a λ or first-order transition were involved. One possible source of difficulty in measurements of this type is nonuniform magnetization introduced by the ends of the sample and indeed our original data (Figs. 2–4) were taken using coils which were roughly the same length as the sample. To investigate this point, we performed a supplementary experiment in which very short coils ($\frac{1}{8}$ in. long, $\frac{5}{16}$ in. o.d.) were used to determine the field dependence of the magnetization at the center of a very long, thin (0.80 in. long, 0.017 in. diam.) niobium sample at 4.2°K. The magnetization was detected by completely removing the sample from the coil in a uniform magnetic field, and observing the deflection of a ballistic galvanometer. The hysteresis which was observed for this sample (Nb-45-1) was less than 0.5% and the locked-in flux was less than 0.3%

[32] J. Matricon, Phys. Letters **9**, 289 (1964).
[33] B. B. Goodman, Phys. Letters **12**, 6 (1964).
[34] T. McConville and B. Serin, Phys. Rev. **140**, A1169 (1965).

of the maximum magnetization. The effects of vibrating the sample were quite small, and one or two excursions of the sample out of the coil brought the sample magnetization to equilibrium. This type of behavior is an indication of a good sample.

An expanded plot of the data taken with this sample at 4.2°K in the region of $H_{c1}$ is shown in Fig. 8. Within the accuracy of the measurements, the magnetization curve shows a complete Meissner effect for $H/H_{c1}<0.93$. At higher fields the magnetization exhibits a long linear region for values of $H/H_{c1}$ from 1.005 to 1.020, during which the magnetization $(-4\pi M/H_{c1})$ decreases from 0.85 to 0.50. This slope (23 G/Oe) is identical with that shown in Figs. 3 and 4. Near the high-field end of this linear region there is a sharp break in the magnetization to a region of much smaller slope, with this smaller slope continuing roughly out to $H_{c2}$, as in Figs. 2 and 3. This knee in the curve may be caused by a transition from the triangular to square array of vortices suggested by Abrikosov,[9] but we have no further evidence that this is the case. The theory predicts this transition at $H/H_{c1}=1.031$ and the observed knee is at $H/H_{c1}=1.025$.

The λ-type transition predicted by the theory[32,33] would produce a magnetization curve similar to the solid line of Fig. 8. A whole family of curves with different values of $a$ and $c$ in Eq. (6) can be generated and the curve shown ($a=14.0$, $c=-5.15$) is the best fit to our data. There are clear differences between the data and Eq. (6) in all ranges of magnetic field. Detailed measurements have been made on five samples of quality comparable to Nb-45-1 (although only this one series of measurements was with the short coil), and all of these samples show the long linear region with a sharp break at $-4\pi M/H_{c1}=0.42$ and $H/H_{c1}=1.025$. This result is independent of demagnetizing factor, temperature, and end effects. In this conclusion we disagree with the results published by McConville and Serin.[34] The reason for the discrepancy is not known.

These same results can be used to calculate discontinuities in the specific heats. Since the change in the slope of the magnetization curve at a second-order

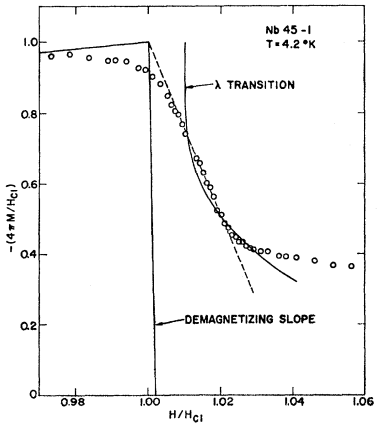


FIG. 8. An expanded presentation of magnetization data for a long, thin sample in the region of $H_{c1}$. The slope and sharp knee at $H/H_{c1}=1.025$ are reproducible from sample to sample. The theoretical curve was calculated from Eq. (6).

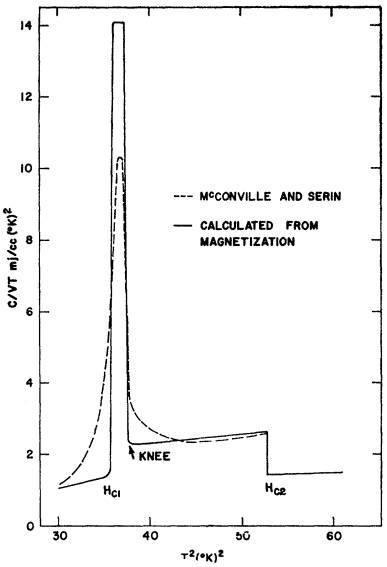


FIG. 9. A comparison of the magnetic data with specific-heat measurements. The calculated specific-heat discontinuities have been shifted arbitrarily to agree with the normal-state data of Boorse *et al.* (Ref. 17).

transition is related to the specific-heat discontinuity at this point by

$$\Delta C=C_1-C_2=-VT(dH_{c1}/dT)^2 \times[(dM/dH)_1-(dM/dH)_2], \quad (7)$$

the magnetization data can be used to calculate the specific-heat differences. In principle, of course, the magnetization data can be used to calculate the entire specific-heat curve, but our data are not sufficiently complete nor sufficiently accurate to allow the necessary integrations and differentiations to be carried out with the required accuracy. It is only in the region of a transition that an accuracy of a few percent can be achieved—and then only in specific-heat differences. The results of these calculations are shown on Fig. 9, where the superconducting specific-heat data of Leupold and Boorse[17] have been assumed below $H_{c1}$, and Eq. (7) has been used to calculate changes in specific heat at $H_{c1}$, at the high-field end of our linear region ($1.025\,H_{c1}$), and at $H_{c2}$. The temperature dependence of the specific heat between these points has been estimated. The jump calculated from the magnetization data at $H_{c1}$ is somewhat higher than the peak observed in the calorimetric work, but the total entropy change is roughly the same.[34] The magnitude of the jump in the specific heat at $H_{c2}$ is in excellent agreement with the calorimetric data.[34]

### The Upper Critical Field $H_{c2}$

The theories of type-II behavior are most reliable in the region of $H_{c2}$. Here the order parameter is vanishingly small and the linear form of the Ginzburg-Landau equations apply. Abrikosov[9] and Tinkham[35] have shown that the upper critical field is related to the penetration depth $\lambda(T)$ and the thermodynamic critical

[35] M. Tinkham, Phys. Rev. **129**, 2413 (1963).

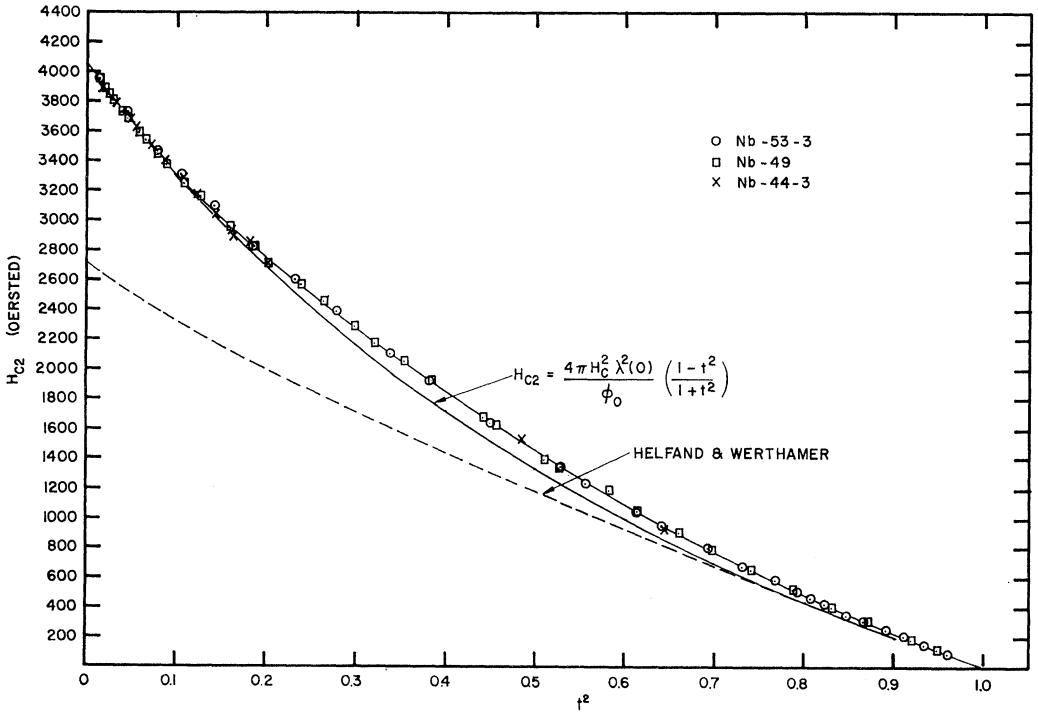


FIG. 10. The upper critical field ($H_{c2}$) of niobium. The solid line represents the relationship $H_{c2}=4040(1-t^2)/(1+t^2)$ which is expected from the Gorter-Casimir theory [Eq. (9)]. The dashed line is given by the theory of Helfand and Werthamer (Ref. 14).

field $H_c$ by

$$H_{c2}=4\pi\lambda^2(T)H_c^2(T)/\varphi_0, \tag{8}$$

where $\varphi_0=2.07$ G cm$^2$ is the flux quantum. This rather general relationship in the framework of the theory requires only that the transition be of second order, a condition which certainly is satisfied for niobium. Since $H_{c2}$, $H_c$, and $\lambda$ are all experimentally determined quantities, a fit of the data to Eq. (8) provides a good test for the GLAG approach in a limit where it should be valid.

The data for $H_{c2}$ shown in Fig. 10 [and tabulated as $(H_{c2}/H_c)=\sqrt{2}\kappa_1$ in Table III] do not fit any existing theory of superconductivity nor indeed do they fit any simple analytic function. In the Gorter-Casimir theory, $\lambda=\lambda(0)(1-t^4)^{-1/2}$ and $H_c=H_0(1-t^2)$, so the upper critical field should be of the form[35]

$$H_{c2}=\frac{4\pi H_c^2\lambda^2(0)}{\varphi_0}\frac{(1-t^2)}{(1+t^2)}. \tag{9}$$

This is shown by the solid line in Fig. 10. Since all superconductors are known to deviate substantially from this model, it is not surprising that this curve differs from the measurements by 8%. Helfand and Werthamer[14] recently have calculated $H_{c2}$ in terms of $H_c$ without recourse to the penetration depth, but their results (shown by the dashed line in Fig. 10) lie somewhat below the measured values. The type of discrepancy which we find here agrees with that reported by Ohtsuka in his magnetocaloric measurements on niobium.[36]

A more fruitful manner of discussing these data is to use the measured values of $H_c$ and $H_{c2}$ in conjunction with Eq. (8) to calculate a penetration depth. The results for Nb-53-3 are plotted versus the usual Gorter-Casimir parameter $y=(1-t^4)^{-1/2}$ in Fig. 11.[1] Near $T_c(y>2)$ the penetration depth closely obeys the usual $\lambda=\lambda(0)/(1-t^4)^{1/2}$ law but at lower temperatures it deviates below this relationship by approximately one-half the amount predicted by the BCS theory (dashed curve, Fig. 11).[29] This is surprisingly close to the behavior of type-I superconductors. In fact, if the penetration depth of tin[37] is scaled to fit niobium near $T_c$, the two curves differ by less than 5% over the entire temperature range. At absolute zero, the magnetization data give $\lambda(0)=410(\pm10)$ Å, which is to be compared with the direct measurement of $470(\pm50)$ Å by Maxfield and McLean.[38] In view of the theoretical uncertainties in Eq. (8) and the difficulty of obtaining an absolute value for $\lambda(0)$ directly, this is rather good agreement.

Another feature of the Abrikosov model which can be tested with these results is the slope of the mag-

[36] T. Ohtsuka, Phys. Letters **17**, 194 (1965).
[37] A. L. Schawlow and G. E. Devlin, Phys. Rev. **113**, 120 (1959).
[38] B. W. Maxfield and W. L. McLean, Phys. Rev. **139**, A1515 (1965).

netization curve at $H_{c2}$. The theory gives for a square array of vortices[13]

$$dM/dH|_{H_{c2}}=[4\pi\cdot 1.18(2\kappa_2^2-1)]^{-1}. \quad (10)$$

The smoothed experimental slopes are given in Table III as a function of $t^2$, together with values of $\kappa_2$ which are defined in Eq. (10). The original Abrikosov theory assumed that $\kappa_2=\kappa_1=H_{c2}/\sqrt{2}H_c=\kappa$ and was a constant independent of temperature. Experimentally and theoretically it is only at $T_c$ that $\kappa_1=\kappa_2$, and this common limiting value at $T_c$ is designated as $\kappa$. The slope of the $\kappa_2/\kappa$-versus-$t$ curve at $t=1$ can be calculated from the results of Neumann and Tewordt[14] as $d(\kappa_2/\kappa)/dt=-1.14$. This is appreciably smaller than our observed value of $d(\kappa_2/\kappa)dt=-2.8$ at $T_c$. This conclusion agrees with that reached by Neumann and Tewordt from a comparison with the heat-capacity data[34] which, as we stated earlier, give values of $dM/dH$ [calculated from Eq. (7)] in excellent agreement with our magnetic values. The discrepancy between theory and experiment for $H_{c2}(t)$ shown in Fig. 10 can be stated also in terms of a discrepancy between experimental and calculated values of $\kappa_1(t)$. In the high-temperature limit, the calculated slope $d(\kappa_1/\kappa)dt$ again is appreciably smaller than the observed slope.[14,36] These discrepancies in both $\kappa_1$ (the magnitude of $H_{c2}$) and $\kappa_2$ (the shape of the magnetization curves at $H_{c2}$) would appear to denote a fundamental difficulty in the theory.

Thus, one can verify that the Abrikosov theory applies only for the case where the energy gap is vanishingly small. It can predict $H_{c2}(T)$ given the experimental values of $H_c(T)$ and a reasonable choice of the penetration depths $\lambda$, and it can predict $dM/dH$ in the limit of high temperatures. It cannot, however, describe the detailed shape of the magnetization curves at lower temperatures. In particular, the type of relationship between $H_c$, $H_{c1}$, and $H_{c2}$ proposed by Harden and Arp[39] (and based on this theory) is not followed by our data, which show a much weaker dependence of $H_{c1}$ on $H_{c2}$.

Since the theory is successful in a limited range of temperature and magnetic field, the magnetization data in this region can be used to calculate other microscopic parameters. The BCS expression for $\lambda_L$ and $\xi_0$ in terms of $\lambda$[28] can be combined self-consistently with the Gor'kov expression

$$\kappa_1=H_{c2}/\sqrt{2}H_c=0.96\lambda_L(0)/\xi_0,$$

to give $\lambda_L(0)=350$ Å and $\xi_0=430$ Å. In addition, the average Fermi velocity can be calculated from the BCS expression

$$\xi_0=0.18\hbar v_F/kT_c$$

to be $3\times10^7$ cm/sec. This rather low value for $v_F$ is not too surprising in view of the important role of the "$d$ bands" for niobium. Presumably the intrinsic type-II character arises in this case because of the high critical temperature and relatively low Fermi velocity.

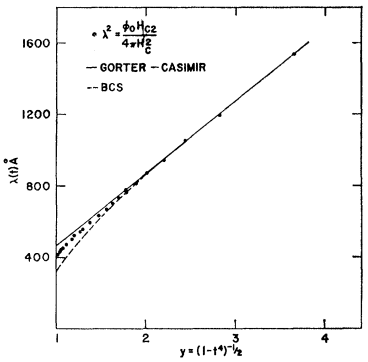


FIG. 11. The penetration depth $\lambda(t)$ for niobium as calculated from the magnetization data using Eq. (8).

### Surface Superconductivity

Saint-James and de Gennes[40] have predicted the existence of a surface superconductivity at fields greater than $H_{c2}$. According to this theory, when a magnetic field is parallel to a vacuum-superconductor interface of radius of curvature greater than $\xi$, a superconducting layer approximately one coherence distance thick should persist up to a field $H_{c3}=1.695H_{c2}$. A large body of experimental work has shown that this layer exists for both type-II[41–43] and type-I[44] superconductors. Since our magnetization measurements do not have the sensitivity required to detect such a layer, we have made preliminary resistance and ac susceptibility measurements on some of our samples. The surface of these samples is thermally etched when the sample is held for an hour or more at temperatures close to the melting point in a vacuum of $10^{-9}$ Torr. Optical observations show that the surfaces are very smooth on a 1 $\mu$ scale with gradual undulations approximately 0.1 mm apart.

Two distinct geometries are possible for these measurements on our typically long, small-diameter wires; the external field either can be parallel or perpendicular to the measuring current density $J$. For the case where $H$ is parallel both to $J$ and to the surface, the resistance was measured directly with a standard four-probe technique. Since the normal state resistance of the best samples was $3\times10^{-6}$ Ω and the measuring current had to be less than $10^{-3}$ A (to give $J\leq2\times10^3$ A/cm² in the surface layer),[15] it was necessary to use an ac method to measure the small voltage changes involved (roughly $10^{-9}$ V) with a few percent precision. A 33-cps

[39] J. L. Harden and V. Arp, Cryogenics 3, 105 (1963).

[40] D. Saint-James and P. G. de Gennes, Phys. Letters 7, 306 (1963).

[41] C. F. Hempstead and Y. B. Kim, Phys. Rev. Letters 12, 145 (1964).

[42] W. J. Tomash and A. S. Joseph, Phys. Rev. Letters 12, 148 (1964).

[43] M. Strongin, A. Paskin, D. G. Schweitzer, O. F. Kammerer, and P. P. Craig, Phys. Rev. Letters 12, 442 (1964); Phys. Rev. 136, A926 (1964).

[44] B. Rosenblum and M. Cardona, Phys. Letters 9, 220 (1964).

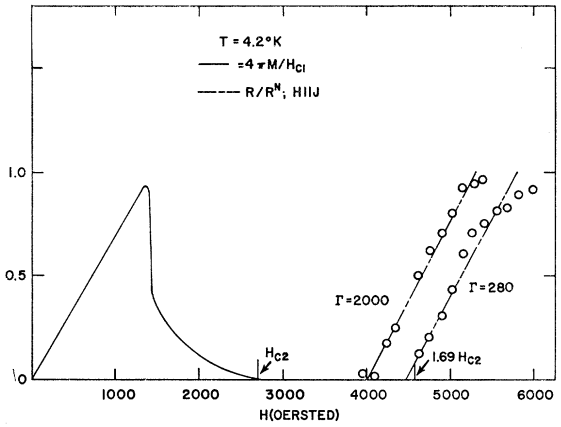


FIG. 12. Resistive transitions for niobium for magnetic field $H$ parallel to the current $J$.

current (low frequency to avoid skin effect difficulties) was sent through the sample and the voltage drop was measured by a 630:1 transformer–narrow-band amplifier–phase-sensitive detector combination. A relatively low-homogeneity superconducting solenoid was used to obtain the 10kG needed for all of these 4.2°K measurements.

Figure 12 shows the magnetic-field dependence of the electrical resistance at 4.2°K for two samples which have resistivity ratios of 280 and 2000, respectively. A typical 4.2°K magnetization curve taken on another sample is shown also. The resistance rise occurs near 1.69 $H_{c2}$ but the transitions are broad and sensitive to sample purity. The measuring currents for these data were less than $10^{-3}$ A, and other data (not shown) indicated that the resistive transition takes place at lower fields as the measuring current is increased until at a current of 0.1 A (roughly at $J=2.5\times10^5$ A/cm$^2$) full restoration is found at $H_{c2}$.

For the case where the measuring current density $J$ is parallel to the surface but perpendicular to the applied field, ac currents were induced around the cylinder and the real $\chi'$ and imaginary $\chi''$ components of the susceptibility were measured. Two different types of mutual-inductance bridge (either a Hartshorn or a ratio-transformer type) were used with modulating fields of less than 1.0 Oe. Unfortunately the susceptibility results were not completely reproducible, and no determined effort was made to discover the source of the irreproducibility. Figure 13 shows the results obtained for two samples at 4.2°K and a third sample at 8°K. Nb-53-2 and Nb-53-3 are two sections of the same sample with very similar resistivity ratios (1670 and 1490) and yet the shapes of the curves are quite different even though indications of $H_{c1}$, $H_{c2}$, and $H_{c3}$ are quite clear in each case. We do not know whether this is a fault due to the sample alignment being different in the two cases, or is due to hysteresis. The ratio of $H_{c3}/H_{c2}$ is close to 1.69. The curve for Nb-44-2 at 8°K shows behavior similar to that of a pure type-I superconductor. There is an apparent paramagnetic region from $H_{c1}$ to $H_{c2}$ and to an accuracy of 1% in both susceptibility components, there is no sign of superconductivity above $H_{c2}$. The $H_{c3}$ effects which are present at 4.2°K are not present at 8°K. Rosenblum and Cardona[44] have shown similar behavior in pure lead where the surface state is present below 5.5°K and disappears at higher temperatures. The recent theoretical calculations of Ebneth and Tewordt[45] for the ratio of $H_{c3}/H_{c2}$ do not apply here because the temperatures are well below $T_c$.

Fink[46] has suggested that these surface currents may be a fundamental cause of irreversibility in superconductors. The model predicts that the multiply connected sheath will shield the normal interior against field changes. These very pure niobium samples provide a good test for this model since there are very few flux-pinning sites. Our samples exhibit the surface superconductivity phenomena but no irreversibility near $H_{c2}$ and extremely little irreversibility near $H_{c1}$. Above $H_{c2}$ the magnetization is the normal-state value to an accuracy of 0.1% of the magnetization at $H_{c1}$. The surface currents may play an important role in producing irreversibility but a defect structure also is required. The flux seems to move freely through the sheath to establish thermodynamic equilibrium.

## IV. CONCLUSION

These experiments give definitive evidence that niobium is an intrinsic type-II superconductor. The zero magnetic-field properties of niobium in the superconducting state are those which might have been expected from the ratio of $T_c/\Theta_D$; niobium is an intermediate-coupling superconductor with a thermodynamic critical-

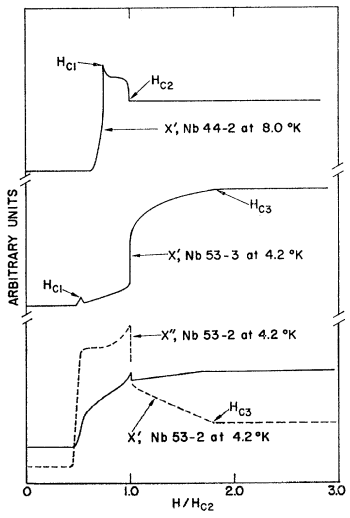


FIG. 13. The ac susceptibility of very pure niobium at 33 cps. The resistivity ratios of the samples are approximately 1600.

[45] G. Ebneth and L. Tewordt, Z. Physik **185**, 421 (1965).
[46] H. J. Fink, Phys. Letters **19**, 364 (1965).

field curve which, on a reduced scale, lies midway between tin and mercury.[47] It is interesting that the surface free-energy effects which play such a large role in determining the shapes of magnetization curves appear to have no effect on the bulk (that is, $H=0$) thermodynamic properties of a superconductor.

The phase transition at $H_{c1}$ is second order and does not appear to be of a $\lambda$ type. The shape of the magnetization curves is very reproducible from sample to sample and is independent of demagnetizing factor and end effects. None of the reversible curves are consistent with a $\lambda$ transition at $H_{c1}$. The phase transition at $H_{c2}$ is second order and the measured slope of the magnetization curve agrees well with values calculated from the specific-heat data. Data taken at 4.2°K show a zero-resistance state which corresponds to the surface superconductivity discussed by Saint-James and de Gennes.[40] For our very pure samples, this multiply connected sheath does not by itself cause irreversibility in the bulk magnetization, but, to the accuracy of these measurements, thermodynamic equilibrium is maintained.

In the region where the GLAG theory is applicable (small energy gap), theory predicts the critical-field behavior of niobium very well. It gives the measured values of $H_{c2}$ for a reasonable choice of the penetration depth and in the limit of temperatures close to $T_c$ it gives a slope for the magnetization curve which approaches the measured slope. The range of validity of this theory is quite limited, however, and quantitative predictions for the shapes of the magnetization curves do not apply for niobium.

It is of interest to compare these conclusions with results for other intrinsic type-II superconductors. Of the other transition metals which can be obtained in high-purity form and which have relatively high $T_c$'s tantalum definitely is a type-I superconductor with an intrinsic (extrapolated) value of $\kappa_1$ at $T_c$ of 0.4.[48] Relatively high purity vanadium shows type-II behavior,[5] as is evident from specific-heat work by Radebaugh and Keesom,[49] and magnetization studies by Martin and Rose-Innes.[50] The specific-heat data in particular (which were taken on a sample with $\Gamma=150$) agree with our general conclusion that the theories of type-II behavior do not apply in the intrinsic limit except near $T_c$.[51] Magnetization data for vanadium which are comparable with those presented here would be of interest, but there are major difficulties in preparing high-purity (that is, high-$\Gamma$) vanadium which are directly associated with the extreme volatility of this metal near its melting point. We have not been able to obtain vanadium metal which is comparable with our niobium.

[47] R. W. Shaw, D. E. Mapother, and D. C. Hopkins, Phys. Rev. **120**, 88 (1960).

## ACKNOWLEDGMENTS

The authors are indebted to many others for assistance in the course of this work. Dr. W. DeSorbo of the General Electric Research Laboratory supplied us with some early material, and Dr. R. J. Wasilewski of the Dupont Corporation made available to us the rather unique low tantalum starting material upon which these results are based. The fabrication was carried out with the assistance of Professor O. N. Carlson and F. A. Schmidt of the Ames Laboratory Metallurgy Division. Many analyses were performed by the Ames Laboratory Spectroscopic Services Group. We would like to acknowledge valuable discussions with Professor B. Serin and with Dr. Y. B. Kim, among others.

[48] J. Buchanan, G. K. Chang, and B. Serin, J. Phys. Chem. Solids **26**, 1183 (1965).

[49] P. H. Keesom and Ray Radebaugh, Phys. Rev. Letters **13**, 685 (1964).

[50] R. B. Martin and A. C. Rose-Innes, Phys. Letters **19**, 467 (1965).

[51] Ray Radebaugh and P. H. Keesom, preceding paper, Phys. Rev. **149**, 217 (1966).